Dalton Transactions

PAPER

View Article Online
View Journal | View Issue

Cite this: *Dalton Trans.*, 2014, **43**, 4871

A copper complex supported by an N_2S-tridentate ligand inducing efficient heterolytic O–O bond cleavage of alkylhydroperoxide†

Tetsuro Tano,[a] Kaoru Mieda,[b] Hideki Sugimoto,[a] Takashi Ogura[b] and Shinobu Itoh*[a]

Received 19th October 2013,
Accepted 9th January 2014

DOI: 10.1039/c3dt52952e

www.rsc.org/dalton

We have recently reported a copper(II)-superoxide complex supported by an N_3-tridentate ligand (L^{N3}), which exhibits a similar structure and reactivity to those of a putative reactive intermediate involved in the catalytic reactions of copper monooxygenases such as peptidylglycine α-hydroxylating monooxygenase (PHM) and dopamine β-monooxygenase (DβM). In this study, we have synthesised and characterised copper complexes supported by a related sulphur-containing ligand (L^{N2S}) to get insight into the notable electronic effect of the sulphur donor atom in the reaction with cumene hydroperoxide, inducing efficient heterolytic O–O bond cleavage.

Introduction

Copper monooxygenases such as peptidylglycine α-hydroxylating monooxygenase (PHM), dopamine β-monooxygenase (DβM) and tyramine β-monooxygenase (TβM) employ two uncoupled, mononuclear copper sites referred to as Cu_M and Cu_H.[1–6] Cu_M serves as the reaction site for dioxygen activation and substrate oxygenation, whereas Cu_H functions as an electron acceptor from the physiological reductant (ascorbate). The Cu_M site is ligated by two histidine imidazoles and one methionine sulphur (N_2S donor set), whereas Cu_H is coordinated by three histidine imidazoles (N_3 donor set).[3,4] These coordination environments are somewhat unusual, since most of the reaction centres of O_2-activating copper proteins (type-2 and type-3 Cu proteins) consist of nitrogen rich donor sets, whereas the large number of electron transfer proteins (type-1 Cu proteins) involve a sulphur-containing ligand environment.[7,8] Thus, such a unique feature of these copper monooxygenases has long been a target in synthetic bioinorganic modelling studies.[9–20]

So far, a series of mononuclear copper–dioxygen adducts have been characterised as model compounds of possible reactive intermediates of copper monooxygenases.[21–25] Among them, a mononuclear copper(II)-superoxide complex supported by a simple N_3-ligand L^{N3} (1-[2-(2-pyridyl)ethyl]-1,5-diazacyclooctane derivatives, Fig. 1) is a unique example, which exhibits both a similar structural feature (distorted tetrahedral copper(II) with an end-on superoxide ligand) and a reactivity (aliphatic hydroxylation) to those of the putative reactive intermediate involved in the enzymatic reactions.[26,27] In this study, we have synthesised and characterised the copper(I) and copper(II) complexes supported by L^{N2S} (Fig. 1) in order to get insights into the effects of the sulphur atom on the structure and reactivity. Ligand L^{N2S} has the same molecular framework as that of L^{N3}, but one of the alkylamine nitrogen atoms is replaced by a sulphur atom, allowing us to simply access the electronic effects of the donor atoms.

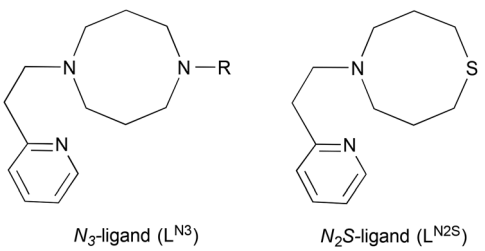

Fig. 1 Ligand structures.

Results and discussion

Synthesis and characterization

The ligand L^{N2S} was synthesized in three steps as shown in Scheme 1. Treatment of 2-(2-aminoethyl)pyridine and 3-chloro-1-propanol in CH_3CN gave a bis(3-hydroxypropyl)-

[a]*Department of Material and Life Science, Division of Advanced Science and Biotechnology, Graduate School of Engineering, Osaka University, 2-1 Yamada-oka, Suita, Osaka 565-0871, Japan. E-mail: shinobu@mls.eng.osaka-u.ac.jp*
[b]*Research Institute of Picobiology, Graduate School of Life Science, University of Hyogo, 3-2-1 Kouto, Kamigori-cho, Ako-gun, Hyogo 678-1297, Japan*

† Electronic supplementary information (ESI) available: Experimental procedures and characterization details. CCDC 959052–959056. For ESI and crystallographic data in CIF or other electronic format see DOI: 10.1039/c3dt52952e

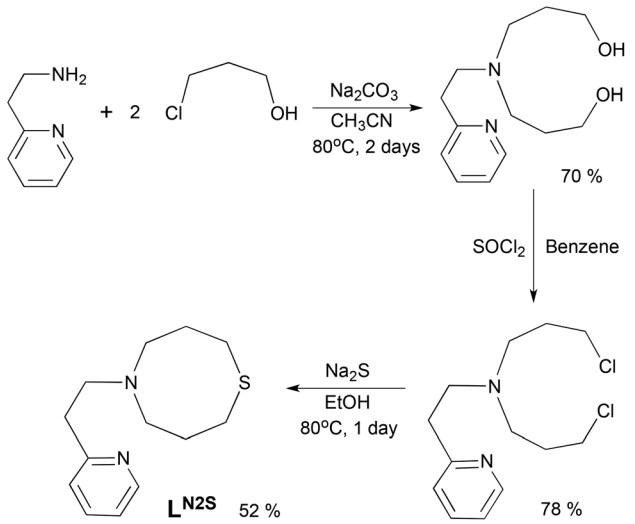

Scheme 1 Ligand synthesis.

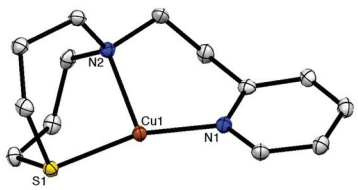

Fig. 2 ORTEP drawing of $\mathbf{1}^{\mathbf{N2S}}$ showing 50% probability thermal ellipsoids. Counter anion (PF_6^-) and hydrogen atoms are omitted for clarity. Cu(1)–S(1), 2.2028(4) Å; Cu(1)–N(1), 1.9295(13) Å; Cu(1)–N(2), 2.1662(13) Å; S(1)–Cu(1)–N(1), 163.02(4)°; S(1)–Cu(1)–N(2), 94.37(4)°; N(1)–Cu(1)–N(2), 102.60(6)°.

amine derivative, which was then converted to the dichloro derivative by the reaction with $SOCl_2$. Ring closure using Na_2S gave the ligand L^{N2S} in a moderate yield.

The copper(I) complex $[Cu^{I}(L^{N2S})](PF_6)$ ($\mathbf{1}^{\mathbf{N2S}}$) was prepared by treating L^{N2S} with an equimolar amount of $[Cu^{I}(CH_3CN)_4](PF_6)$ in THF. The crystal structure of $\mathbf{1}^{\mathbf{N2S}}$ is shown in Fig. 2. The crystallographic data and the selected bond lengths and angles of $\mathbf{1}^{\mathbf{N2S}}$ are presented in Table S1† and the figure caption, respectively. $\mathbf{1}^{\mathbf{N2S}}$ exhibits a slightly distorted T-shaped structure ligated by the two nitrogen atoms N(1) and N(2), and one sulphur atom S(1) of the supporting ligand. The sum of the three angles around the copper center [∠S(1)–Cu(1)–N(1), ∠S(1)–Cu(1)–N(2), ∠N(1)–Cu(1)–N(2)] is equal to 360°, indicating that the copper ion and the three donor atoms exist in the same plane. The copper(I) complex $\mathbf{1}^{\mathbf{N3}}$ supported by L^{N3} exhibited a similar T-shaped structure, demonstrating that the molecular framework of the ligands can highly stabilise such a three coordinate T-shaped structure of copper(I).[26,27] Although the precise structure of the reduced enzyme is not known, the EXAFS data have suggested that the reduced Cu_M is 3-coordinate, or 4-coordinate with a weakly bound water molecule, where the Cu_M–S_{Met} distance is 2.24 Å.[4] In this context, $\mathbf{1}^{\mathbf{N2S}}$ represents a good structural model of

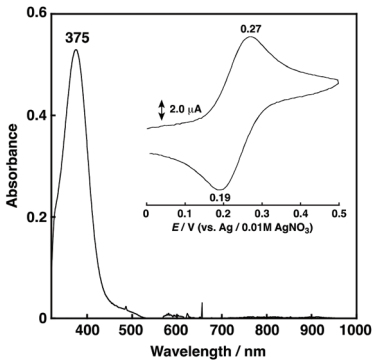

Fig. 3 UV-vis spectrum of $\mathbf{1}^{\mathbf{N2S}}$ (0.5 mM) in acetone at 25 °C. Inset: cyclic voltammogram of $\mathbf{1}^{\mathbf{N2S}}$ (1.0 mM) in acetone containing 0.1 M $TBAPF_6$; working electrode GC, counter electrode Pt, reference electrode Ag/0.01 M $AgNO_3$, scan rate 50 mV s^{-1}.

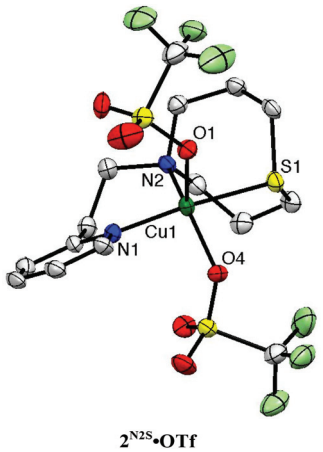

$\mathbf{2}^{\mathbf{N2S}}\cdot\mathbf{OTf}$

Fig. 4 ORTEP drawings of $\mathbf{2}^{\mathbf{N2S}}\cdot\mathbf{OTf}$ showing 50% probability thermal ellipsoids. Hydrogen atoms are omitted for clarity. Cu(1)–S(1), 2.2860(15) Å; Cu(1)–O(1), 2.247(4) Å; Cu(1)–O(4), 2.118(4); Cu(1)–N(1), 2.006(5) Å; Cu(1)–N(2), 2.040(6) Å; S(1)–Cu(1)–O(1), 84.84(11)°; S(1)–Cu(1)–O(4), 84.78(12)°; S(1)–Cu(1)–N(1), 171.15(16)°; S(1)–Cu(1)–N(2), 90.42(14)°; O(1)–Cu(1)–O(4), 95.93(15)°; O(1)–Cu(1)–N(1), 92.12(16)°; O(1)–Cu(1)–N(2), 109.86(17)°; O(4)–Cu(1)–N(1), 87.27(18)°; O(4)–Cu(1)–N(2), 153.25(16)°; N(1)–Cu(1)–N(2), 98.4(2)°.

reduced Cu_M, even though the Cu–S distance in $\mathbf{1}^{\mathbf{N2S}}$ (2.203 Å) is slightly shorter than that in the enzyme (2.24 Å).

$\mathbf{1}^{\mathbf{N2S}}$ showed a relatively intense absorption band at 375 nm (ε = 1058 M^{-1} cm^{-1}) ascribable to a Cu^{I} to S charge transfer (MLCT) (Fig. 3), and exhibited a reversible Cu^{I}/Cu^{II} redox couple at 0.23 V *vs.* $Ag/AgNO_3$ in acetone (Fig. 3, inset) that is higher than that of $\mathbf{1}^{\mathbf{N3}}$ (0.11 V for R = $-CH_2CH_2Ph$) under the same conditions.[27]

Copper(II) complexes $\mathbf{2}^{\mathbf{N2S}}\cdot\mathbf{X}$ (X = coordinating counter anion; Cl, N_3, NO_2, OTf) were also prepared as the model compounds of resting enzymes in the copper(II) oxidation state. The crystal structures of $\mathbf{2}^{\mathbf{N2S}}\cdot\mathbf{Cl}$, $\mathbf{2}^{\mathbf{N2S}}\cdot\mathbf{N_3}$, $\mathbf{2}^{\mathbf{N2S}}\cdot\mathbf{NO_2}$ and $\mathbf{2}^{\mathbf{N2S}}\cdot\mathbf{OTf}$ have been determined as shown in Fig. S1, S2,† and Fig. 4. The crystallographic data and the selected bond lengths and angles are summarised in Tables S2 and S3,† respectively.

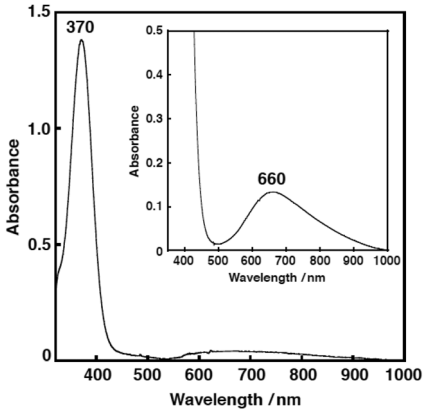

Fig. 5 The UV-vis spectrum of $\mathbf{2^{N2S}}$**·OTf** (0.25 mM) in acetone, at −85 °C. λ_{max} = 370 nm (ε = 5520 M^{-1} cm^{-1}). Inset: an expanded UV-vis spectrum of $\mathbf{2^{N2S}}$**·OTf** (0.60 mM). λ_{max} = 660 nm (ε = 222 M^{-1} cm^{-1}).

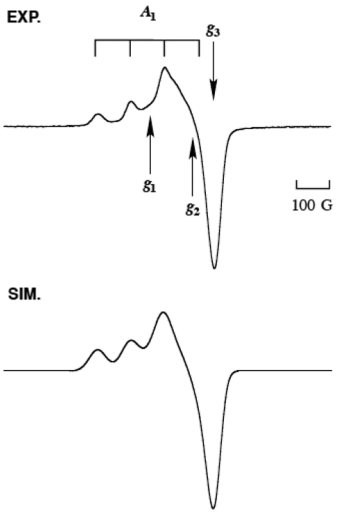

Fig. 6 The EPR spectrum (EXP, top) of $\mathbf{2^{N2S}}$**·OTf** (0.5 mM) in acetone at −196 °C, and its computer simulation spectrum (SIM, bottom) with the parameters of g_1 = 2.275, g_2 = 2.100, g_3 = 2.015, A_1 = 150 G, A_2 = 59 G, and A_3 = 16 G.

All the copper(II) complexes exhibit five-coordinate structures with τ = 0.01–0.55,[28] among which $\mathbf{2^{N2S}}$**·Cl** and $\mathbf{2^{N2S}}$**·N$_3$** form coordination polymer chain structures, where the coordinating counter anion (Cl^- and N_3^-) acts as the bridging ligand (Fig. S1†). On the other hand, $\mathbf{2^{N2S}}$**·OTf** and $\mathbf{2^{N2S}}$**·NO$_2$** exhibit a monomeric structure as shown in Fig. 4 and Fig. S2.† Thus, the structure and chemical properties were examined using $\mathbf{2^{N2S}}$**·OTf** in more detail.

The copper(II) complex $\mathbf{2^{N2S}}$**·OTf** exhibits a distorted square pyramidal structure coordinated by N(1), N(2), S(1) and O(4) in the equatorial plane and O(1) occupying the axial position (τ = 0.30), which is in accord with the observed ligand field absorption band at 660 nm (ε = 222 M^{-1} cm^{-1}, Fig. 5) and a typical EPR signals of Cu^{II} with a tetragonal geometry (Fig. 6, the EPR parameters are provided in the figure caption). The structural feature is quite different from that of the copper(II) complexes supported by L^{N3}, which enforces the copper(II) center having a four-coordinate distorted tetrahedral geometry.[26,27] Thus, the replacement of the donor atom from nitrogen to sulphur resulted in a significant change in the coordination geometry of the metal center from the four-coordinate distorted tetrahedral to the five-coordinate square pyramid or trigonal bipyramidal. In this case, Cu–S distance is 2.286 Å, which is longer than that in the copper(I) complex (2.203 Å). Such an elongation of the Cu^{II}–S bond demonstrates the strong preference of the Cu^{I}–S bond as compared to the Cu^{II}–S bond. However, the Cu^{II}–S distance in the model complex (2.286 Å) is much shorter than that in the resting state (copper(II) oxidation state) of the enzyme, that is, 2.68 Å, although the coordination geometries are similar to each other.[3]

Reactivity

First, the reaction of $\mathbf{1^{N2S}}$ and O_2 was examined in acetone at low temperature (−85 °C). However, no spectral change was observed. Even at room temperature or in other solvents such as THF and CH_2Cl_2, $\mathbf{1^{N2S}}$ showed no reactivity toward O_2. This result is in sharp contrast to the high O_2-reactivity of $\mathbf{1^{N3}}$, which gives a mononuclear copper(II)-superoxide complex.[26,27] Such a big difference in the O_2-reactivity between the two ligand systems could be attributed to the higher oxidation potential of $\mathbf{1^{N2S}}$ (0.23 V) as compared to that of $\mathbf{1^{N3}}$ (0.11 V). As mentioned above, the Cu–S distance in the enzyme is much longer, especially in the copper(II) oxidation state, which may cause the less copper(I)-stabilizing effect of the sulphur donor atom in the enzymatic system. Therefore, Cu_M may be able to activate O_2 for the substrate oxygenation reaction even in the presence of the Met ligand.

On the other hand, $\mathbf{1^{N2S}}$ smoothly reacted with cumene hydroperoxide (CmOOH) in a 1 : 1 ratio to give CmOH (cumyl alcohol) as the major product (98%) together with a trace amount of acetophenone (PhC(O)Me), where CmOOH was completely consumed (Fig. S3†). In the case of $\mathbf{1^{N3}}$, on the other hand, only 44% of CmOH was obtained together with a small amount of PhC(O)Me (6%), and 50% of CmOOH was recovered (Fig. S4†). Thus, the stoichiometry in the $\mathbf{1^{N3}}$ case was 2 : 1.

We have recently examined the reactivity of a series of copper complexes using CmOOH as a proof for searching the O–O breaking pattern in the copper-peroxide adducts.‡[29,30] It has been demonstrated that copper(I) complexes supported by nitrogen ligands react with CmOOH in a 2 : 1 ratio to induce the heterolytic O–O bond cleavage of the peroxide to give CmOH as the major product. In this case, each copper(I)

‡It has been reported that the products obtained from a cumylperoxo complex largely depend on the O–O bond cleavage pattern. If homolytic O–O bond cleavage occurs, acetophenone (PhCOMe) is produced from cumyloxyl radical *via* β-scission releasing methyl radical ($CH_3^•$). In contrast, heterolytic O–O bond cleavage gives cumyl alcohol (CmOH) after oxyanion protonation.[36,37]

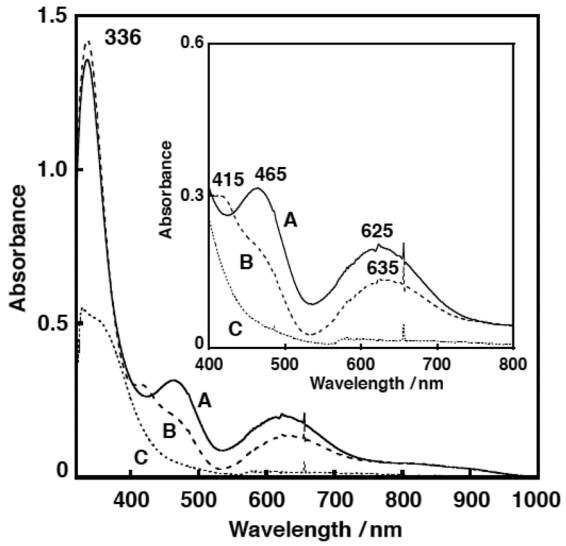

Fig. 7 The UV-vis spectra of intermediate **A** (solid line; 1000 s after the reaction of $\mathbf{1}^{N2S}$ (0.5 mM) with an equimolar amount of CmOOH in acetone at −85 °C), **B** (dashed line; 1 h after the reaction), and **C** (dotted line; after warming to 30 °C). Inset: expanded spectra at the 400–800 nm region.

complex formally acts as a one-electron donor to induce total two-electron reduction of CmOOH, thus providing the heterolytic cleavage product, CmOH, in a ~50% yield based on the copper(I) starting material (stoichiometry of Cu : CmOOH is 2 : 1).[30] Thus, $\mathbf{1}^{N3}$ (N_3-donor ligand) giving CmOH in a ~50% yield is involved in this category.

In this respect, the reactivity of $\mathbf{1}^{N2S}$ (N_2S-donor ligand) is different, showing the 1 : 1 stoichiometry to give CmOH in a ~100% yield based on the copper(I) starting material. Such a unique reactivity of $\mathbf{1}^{N2S}$ can be attributed to the presence of the sulphur atom. In order to get insight into the effect of the sulphur atom, the reaction was examined by UV-vis, resonance Raman and EPR spectra as follows.

Fig. 7 shows the UV-vis spectral change for the reaction of $\mathbf{1}^{N2S}$ and an equimolar amount of CmOOH in acetone. After about 1000 s, an intermediate **A** exhibiting characteristic absorption bands at 336, 465 and 625 nm was developed (Fig. 7, solid line). This intermediate was gradually converted to another intermediate **B** having absorption bands at 336, 415, and 635 nm (Fig. 7, dashed line). When the solution was warmed to room temperature, the absorption bands in the visible region disappeared, suggesting formation of a copper(I) product **C** (Fig. 7, dotted line). The EPR spectrum of the final reaction solution was essentially EPR silent, being consistent with the formation of a copper(I) complex (Fig. S8†).

Then, the reaction was examined by resonance Raman spectrum at the low temperature. As shown in Fig. S5,† isotope-sensitive Raman bands were observed at 887, 827 and 610 cm^{-1}, which shifted to 794 and 603 cm^{-1}, when ^{18}O-labeled CmOOH was employed. The Raman bands at 887 and 827 cm^{-1} could be attributed to the O–O bond stretching vibration of a cumylperoxide adduct intermediate **A** and the band at 610 cm^{-1} may be due to the Cu–O stretching vibration.§[31]

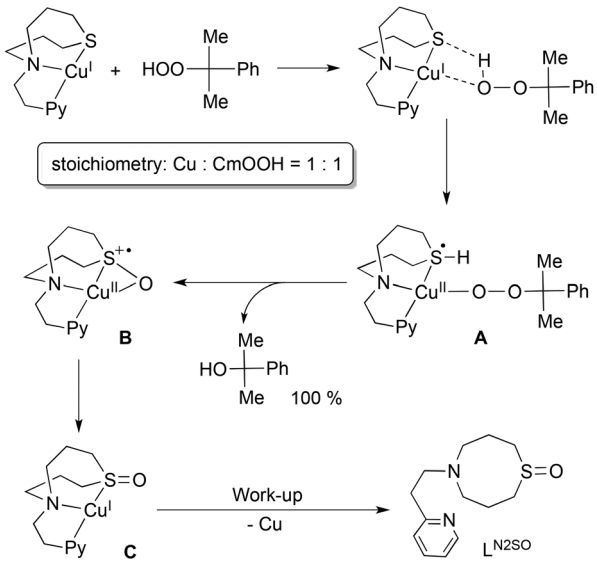

Scheme 2

On the basis of these results, a possible reaction mechanism is proposed in Scheme 2. Association of the copper(I) complex $\mathbf{1}^{N2S}$ and CmOOH may induce proton-coupled electron-transfer (PCET) to generate intermediate **A**, where a proton of CmOOH is transferred to the sulphur atom and an electron is transferred from copper(I) to the sulphur atom. In this case, an empty d orbital of the sulphur atom can accommodate the electron provided from copper(I). Then, nucleophilic attack of the sulphur atom to the proximal oxygen leads to S–O bond formation with concomitant proton migration to the distal oxygen atom. Eventually, O–O bond heterolytic cleavage takes place to give intermediate **B** and CmOH. Then, electronic rearrangement of **B** occurs upon warming to give a copper(I) complex **C** with an oxygenated ligand.

The sulphoxide ligand L^{N2SO} was obtained nearly quantitatively after the work-up treatment of the reaction mixture with NH_4OH aq (demetalation). The formation of L^{N2SO} was confirmed by ^1H-NMR, IR and ESI-mass spectra (Fig. S5 and S6,† also see the Experimental section), and the isotope labeling experiment using $Cm^{18}O_2H$ confirmed that the oxygen atom incorporated into the ligand originated from the CmOOH used (Fig. S6†). Oxygenated product L^{N2SO} was not obtained at all in the reaction of ligand itself and CmOOH under the same experimental conditions. Although mechanistic details of the enzymatic reaction remain obscure, such a role of sulphur

§ The resonance Raman bands due to the C–C–C and C–C–O deformation modes of the alkylperoxide moiety were also observed at 540, 490 and 436 cm^{-1} in the ^{16}O-derivative (see Fig. S5†). However, their counterparts in the ^{18}O-derivative became obscure due to low quality of the spectrum. The two peaks at 887 and 827 cm^{-1} for the O–O vibration of the ^{16}O-derivative may be Fermi doublet, which collapsed into one peak at 794 cm^{-1} in the ^{18}O-derivative. More detailed examination is required for the complete assignment of the resonance Raman spectrum.

ligand could be involved in enhancing the O–O bond cleavage of the peroxide intermediate in the copper monooxygenases.

Conclusions

In summary, copper(I) and copper(II) complexes of the N_2S ligand (L^{N2S}) have been synthesised and characterised in order to get insights into the effects of the sulphur atom of the Met ligand in the enzyme active site. Structural examinations have suggested that the sulphur coordination in the present model system is stronger than that in the enzymatic system, causing higher stability of the copper(I) oxidation state toward O_2. Nonetheless, a reactivity study using cumen hydroperoxide has clearly indicated that the sulphur atom helps in the O–O bond heterolysis of the peroxide intermediate. Such an effect of sulphur might be important to facilitate the enzymatic reactions. The present result also suggests that the sulphur atom of the Met ligand in the enzymatic system can be oxygenated to sulphoxide during the catalytic cycles. In other words, post-translational modification of the Met sulphur could occur in the enzyme active site.

Experimental section

Materials and physical measurements

The reagents and the solvents used in this study, except the ligands, cumene hydroperoxide and the copper complexes, were commercial products of the highest available purity and were further purified by standard methods, if necessary.[32] Cumene hydroperoxide (CmOOH) used in this study was prepared by a reported procedure,[33] and purified by silica gel column chromatography (eluent: AcOEt–Hexane). ^{18}O-labeled ($Cm^{18}O^{18}OH$) was synthesized using $^{18}O_2$ instead of $^{16}O_2$ by the same procedure.

UV-visible spectra were taken in acetone or in acetonitrile on a Hewlett Packard 8453 photodiode array spectrophotometer equipped with a Unisoku thermostated cell holder designed for low temperature measurements (USP-203). ^{1}H-NMR spectra were recorded on a JEOL ECS 400 or a Varian UNITY INOVA 600 MHz. ESR spectra were recorded on a BRUKER E-500 spectrometer at −196 °C equipped with a variable temperature cell holder or a JEOL JES-FA100. A Mn^{II}-maker was used as the reference, and experimental error in the EPR parameter is ±0.001. Mass spectra were recorded with a JEOL JMS-700T Tandem MS station or a JEOL JMS-700. ESI-MS (electrospray ionization mass spectra) measurements were performed on a Mariner ESI-TOF instrument. Cyclic voltammetric measurements were performed with a Hokuto Denko HZ-3000 or HZ-7000 in deaerated solvent containing 0.10 M n-Bu_4PF_6 as a supporting electrolyte. A GC working (BAS) electrode was polished with BAS polishing alumina suspension and rinsed with acetone before use. The counter electrode was a platinum wire. The measured potentials were recorded with respect to an $Ag/AgNO_3$ (0.01 M) reference electrode.

Resonance Raman scattering was excited 441.6 nm from a He–Cd laser (KIMMON KOHA, K5651R). Resonance Raman scattering was dispersed by a single polychromator (Ritsu Oyo Kogaku, MC-100) and was detected by a liquid nitrogen cooled CCD detector (HORIBA JOBIN YVON, Symphony 1024 × 128 Cryogenic Front Illuminated CCD Detector). The resonance Raman measurements were carried out using a rotated cylindrical cell thermostated at −80 °C or a rotating NMR tube (outer diameter = 5 mm) thermostated at −40 °C by flashing cold nitrogen gas. A 135° back-scattering geometry was used.

Synthesis

***N*-(Pyridine-2-yl)ethyl-bis(3-hydroxypropyl)amine.** A 200 mL round-bottom flask was charged with 2-(2-aminoethyl)pyridine (4.0 g, 33 mmol), 3-chloro-1-propanol (13 g, 0.13 mol), sodium carbonate (35 g, 0.33 mol), tetrabutylammonium bromide (~5 mg), water (70 mL) and CH_3CN (70 mL). The mixture was refluxed for 2 days. The reaction mixture was cooled to room temperature and extracted with $CHCl_3$ (3 × 50 mL), and the combined organic fractions were dried over Na_2SO_4. After removal of Na_2SO_4 by filtration, evaporation of the solvent gave a brown oil, from which the pure product was isolated by alumina column chromatography (eluent: AcOEt–MeOH = 95 : 5) in 70% (6.5 g). ^{1}H-NMR ($CDCl_3$) δ 1.67 (4 H, pentet, J = 6.0 Hz, CH_2–CH_2–CH_2), 2.65 (4 H, t, J = 6.0 Hz, N–CH_2–CH_2–CH_2–OH), 2.82 (2 H, t, J = 7.2 Hz, Py–CH_2–CH_2–), 3.00 (2 H, t, J = 7.2 Hz, Py–CH_2–CH_2–), 3.61 (4 H, t, J = 5.6 Hz, –CH_2–OH), 7.15–7.18 (1 H, m, PyH_5), 7.20 (1 H, d, J = 7.6 Hz, PyH_3), 7.66 (1 H, td, J = 1.6 Hz and J = 7.2 Hz, PyH_4), 8.50 (1 H, d, J = 2.4 Hz, PyH_6); HRMS (EI^+) m/z = 238.1680, calcd for $C_{13}H_{22}N_2O_2$ = 238.1681.

***N*-(Pyridine-2-yl)ethyl-bis(3-chloropropyl)amine.** *N*-(Pyridine-2-yl)ethyl-bis(3-hydroxypropyl)amine (0.36 g, 1.3 mmol) in benzene (30 mL) was cooled to 0 °C. At this temperature, 0.5 mL of thionyl chloride was added dropwise under aerobic conditions. After an initial exothermal reaction, the mixture was refluxed for 4 h, then brought down to room temperature and left to stand overnight. After cooling down again to 0 °C, a solution of sodium carbonate (10%) was poured until the pH became basic. The organic layer was then separated, and dried over Na_2SO_4. After removal of Na_2SO_4 by filtration, evaporation of the solvent gave a brown oil, from which the pure product was isolated by alumina column chromatography (eluent: AcOEt) in 78% (0.28 g). ^{1}H-NMR ($CDCl_3$, 400 MHz) δ 1.84 (4 H, pentet, J = 6.4 Hz, CH_2–CH_2–CH_2), 2.59 (4 H, t, J = 6.4 Hz, N–CH_2–CH_2–CH_2–Cl), 2.84 (2 H, t, J = 6.4 Hz, Py–CH_2–CH_2–), 2.91 (2 H, t, J = 6.4 Hz, Py–CH_2–CH_2–), 3.46 (4 H, t, J = 6.4 Hz, –CH_2–Cl), 7.09–7.13 (1 H, m, PyH_5), 7.19 (1 H, d, J = 8.0 Hz, PyH_3), 7.59 (1 H, td, J = 1.6 Hz and J = 7.6 Hz, PyH_4), 8.53 (1 H, d, J = 4.8 Hz, PyH_6); HRMS (EI^+) m/z = 274.1003, calcd for $C_{13}H_{20}Cl_2N_2$ = 274.1004.

***N*-(2-(Pyridin-2-yl)ethyl)-1-thia-5-azacyclooctane (L^{N2S}).** *N*-(Pyridine-2-yl)ethyl-bis(3-chloropropyl)amine (0.2 g, 0.55 mmol) was combined with Na_2S (43 mg, 0.55 mmol) in anhydrous

ethanol (100 mL) and refluxed for 19 h. The ethanol was then evaporated *in vacuo*. The residue was taken up with Et_2O (50 mL) and washed with 5% NaOH aq (20 mL × 3) and then water, and dried over Na_2SO_4. After removal of Na_2SO_4 by filtration, evaporation of the solvent gave a yellow oil, from which the ligand L^{N2S} was isolated by alumina column chromatography (eluent: AcOEt) in 52% (67 mg). ^{1}H-NMR ($CDCl_3$, 400 MHz) δ 1.81 (4 H, pentet, J = 6.0 Hz, CH_2–CH_2–CH_2), 2.48 (4 H, t, J = 6.0 Hz, –CH_2–N–CH_2–), 2.64 (4 H, t, J = 6.4 Hz, –CH_2–S–CH_2–), 2.87–2.94 (4 H, m, Py–CH_2–CH_2–), 7.10–7.13 (1 H, m, PyH_5), 7.17 (1 H, d, J = 7.6 Hz, PyH_3), 7.60 (1 H, td, J = 2.0 Hz and J = 8.0 Hz, PyH_4), 8.54 (1 H, d, J = 5.2 Hz, PyH_6); HRMS (EI$^+$) m/z = 236.1348, calcd for $C_{13}H_{20}N_2S$ = 236.1347.

[Cu^I(L^{N2S})](PF$_6$) ($\mathbf{1}^{N2S}$). Since the copper(I) complex is sensitive to air, all the manipulations for the synthesis, crystallization, and stock solution preparation of the copper(I) complex were carried out under a N_2 atmosphere inside a glovebox (KOREA KIYON KK-011AS, [O_2] < 1 ppm).

[Cu^I(CH_3CN)](PF$_6$) (24 mg, 64 μmol) was added to a THF solution of L^{N2S} (15 mg, 64 μmol). After stirring the solution for 30 min at room temperature, the insoluble material was removed by filtration. Addition of ether (50 mL) to the filtrate gave yellow-green solids that were isolated by decantation, washed with ether three times, and dried (45% yield, 13 mg). Single crystals were obtained for the X-ray analysis by vapor diffusion of ether into a THF solution of the complex. FT-IR (KBr) 841 cm^{-1} (PF_6^-); ESI-MS (pos.) m/z = 299.3, calcd for [Cu^I(L^{N2S})]$^+$ 299.1; Anal. Calcd for [Cu^I(L^{N2S})]PF_6 ($C_{13}H_{20}CuF_6N_2PS$): C, 35.10; H, 4.53; N, 6.30. Found: C, 35.43; H, 4.64; N, 6.30.

[Cu^{II}(L^{N2S})(OTf)$_2$] ($\mathbf{2}^{N2S}$·OTf). To a CH_2Cl_2 solution of L^{N2S} (8.0 mg, 34 μmol) was added Cu^{II}(OTf)$_2$ (12 mg, 34 μmol). After stirring for 5 min, the insoluble material was then removed by filtration. The filtrate was concentrated to give a green oily material. Single crystals were obtained for the X-ray analysis by diffusion of *n*-hexane into a CH_2Cl_2 solution of the green material (74% yield, 15 mg). FT-IR (KBr) 1262, 1170 and 1035 cm^{-1} (OTf^-); ESI-MS (pos.) m/z = 448.1, calcd for [Cu^{II}(L^{N2S})(OTf)]$^+$ 448.0; Anal. Calcd for Cu^{II}(L^{N2S})(NO_2)(OTf)·0.5H_2O ($C_{14}H_{21}ClCuF_3N_3O_{5.5}S_2$): C, 33.05; H, 3.40; N, 4.71. Found: C, 30.13; H, 3.37; N, 4.68.

Other copper(II) complexes $\mathbf{2}^{N2S}$·**Cl**, $\mathbf{2}^{N2S}$·$\mathbf{N_3}$, and $\mathbf{2}^{N2S}$·$\mathbf{NO_2}$ were prepared in a similar manner, as described in the ESI.†

Product analysis

Decomposition products of cumene hydroperoxide. An acetone solution (3.0 mL) of $\mathbf{1}^{N2S}$ (0.5 mM) was cooled to −85 °C, and then an acetone solution of CmOOH (1 equiv.) was added to the solution under a nitrogen atmosphere. The resulting mixture was stirred for 1 h at −85 °C. After warming the solution to room temperature, anisole (0.5 mM) was added as an internal standard, and then decomposition products derived from cumene hydroperoxide were analyzed by using a HPLC system consisting of a Shimadzu 10A series. Reverse phase chromatography was performed on an ODS column (Cosmosil 5C_{18}-AR-II, 250 mm × 4.6 mm, Nacalai tesque) at room temperature with an acetonitrile–water (40 : 60) mixed solvent as the mobile phase at a constant flow rate of 0.5 mL min^{-1}. The yields of products were determined by comparing the integrated peak areas of the products with that of the internal standard (anisole) using calibration lines.†

Hydroxylated ligand (L^{N2SO}). An acetone solution (3.0 mL) of $\mathbf{1}^{N2S}$ (12 mg, 27 μmol) was cooled to −85 °C using a Unisoku thermostated cell holder designed for low temperature measurement. Then, an acetone solution of CmOOH (2 equiv.) was added to the solution under a nitrogen atmosphere. The resulting mixture was stirred for 1 h at −85 °C, and then gradually warmed to room temperature. A mixture of organic materials was obtained by treating the reaction mixture with an NH_3 aq and subsequent extraction by $CHCl_3$. The combined organic layer was dried over Na_2SO_4. After removal of Na_2SO_4 by filtration, evaporation of the solvent gave a yellow oil. ^{1}H-NMR (400 MHz, $CDCl_3$) δ 2.03 (2 H, pentet, J = 6.0 Hz, CH_2–CH_2–CH_2), 2.18 (2 H, pentet, J = 6.0 Hz, CH_2–CH_2–CH_2–), 2.62 (2 H, m, –CH_2–S–CH_2–), 2.74 (2 H, m, –CH_2–S–CH_2–) 2.77–2.84 (4 H, m, N–CH_2–CH_2–), 3.32 (2 H, m, Py–CH_2–CH_2–), 3.50 (2 H, m, Py–CH_2–CH_2–), 7.16–7.20 (1 H, m, PyH_5), 7.46–7.51 (1 H, m, PyH_3), 7.67 (1 H, td, J = 2.0 Hz and J = 8.0 Hz, PyH_4), 8.54 (1 H, d, J = 5.2 Hz, PyH_6); HRMS (FAB$^+$) m/z = 253.1378, calcd for $C_{13}H_{21}N_2OS$ ([L^{N2SO} + H]$^+$) = 253.1375. FT-IR (neat) 1077, 1104 cm^{-1} (S═O).†

X-ray crystal structure determination†

Each single crystal obtained was mounted on a CryoLoop (Hampton Research Co.) with a mineral oil, and all data of X-ray diffraction were collected at −170 °C on a Rigaku R-AXIS-RAPID diffractometer using filtered Mo-Kα radiation. The structures were solved by direct methods SIR 92 or SIR 2008 and expanded using Fourier techniques.[34,35] The non-hydrogen atoms were refined anisotropically by full-matrix least-squares on F^2. The hydrogen atoms were attached at idealized positions on carbon atoms and were not refined. All structures in the final stages of refinement showed no movement in the atom positions. The calculations were performed using Single-Crystal Structure Analysis Software, version 4.0.

Acknowledgements

This work was supported by a Grant-in-Aid for Scientific Research on Innovative Areas "Molecular Activation Directed toward Straightforward Synthesis" (no. 22105007) and "Stimuli-responsive Chemical Species" (no. 24109015) and a Grant-in-Aid for Exploratory Research (no. 25620044) from the Ministry of Education, Culture, Sports, Science and Technology, Japan.

Notes and references

1 J. P. Klinman, *Chem. Rev.*, 1996, **96**, 2541–2562.

2 S. T. Prigge, R. E. Mains, B. A. Eipper and L. M. Amzel, *Cell. Mol. Life Sci.*, 2000, **57**, 1236–1259.
3 S. T. Prigge, A. S. Kolhekar, B. A. Eipper, R. E. Mains and L. M. Amzel, *Science*, 1997, **278**, 1300–1305.
4 N. J. Blackburn, F. C. Rhames, M. Ralle and S. Jaron, *J. Biol. Inorg. Chem.*, 2000, **5**, 341–353.
5 N. J. Blackburn, S. S. Hasnain, T. M. Pettingill and R. W. Strange, *J. Biol. Chem.*, 1991, **266**, 23120–23127.
6 C. Hess, J. Klinman and N. Blackburn, *J. Biol. Inorg. Chem.*, 2010, **15**, 1195–1207.
7 E. I. Solomon, M. J. Baldwin and M. D. Lowery, *Chem. Rev.*, 1992, **92**, 521–542.
8 E. I. Solomon, F. Tuczek, D. E. Root and C. A. Brown, *Chem. Rev.*, 1994, **94**, 827–856.
9 L. Casella, M. Gullotti, M. Bartosek, G. Pallanza and E. Laurenti, *J. Chem. Soc., Chem. Commun.*, 1991, 1235–1237.
10 G. Alzuet, L. Casella, M. Laura Villa, O. Carugo and M. Gullotti, *J. Chem. Soc., Dalton Trans.*, 1997, 4789–4794.
11 F. Champloy, N. Benali-Cherif, P. Bruno, I. Blain, M. Pierrot, M. Reglier and A. Michalowicz, *Inorg. Chem.*, 1998, **37**, 3910–3918.
12 T. Ohta, T. Tachiyama, K. Yoshizawa, T. Yamabe, T. Uchida and T. Kitagawa, *Inorg. Chem.*, 2000, **39**, 4358–4369.
13 M. Kodera, T. Kita, I. Miura, N. Nakayama, T. Kawata, K. Kano and S. Hirota, *J. Am. Chem. Soc.*, 2001, **123**, 7715–7716.
14 N. W. Aboelella, B. F. Gherman, L. M. R. Hill, J. T. York, N. Holm, V. G. Young, C. J. Cramer and W. B. Tolman, *J. Am. Chem. Soc.*, 2006, **128**, 3445–3458.
15 L. Zhou, D. Powell and K. M. Nicholas, *Inorg. Chem.*, 2006, **45**, 3840–3842.
16 L. Zhou, D. Powell and K. M. Nicholas, *Inorg. Chem.*, 2007, **46**, 7789–7799.
17 Y. Lee, D.-H. Lee, A. A. Narducci Sarjeant, L. N. Zakharov, A. L. Rheingold and K. D. Karlin, *Inorg. Chem.*, 2006, **45**, 10098–10107.
18 L. Q. Hatcher, D. H. Lee, M. A. Vance, A. E. Milligan, R. Sarangi, K. O. Hodgson, B. Hedman, E. I. Solomon and K. D. Karlin, *Inorg. Chem.*, 2006, **45**, 10055–10057.
19 D.-H. Lee, L. Q. Hatcher, M. A. Vance, R. Sarangi, A. E. Milligan, A. A. Narducci Sarjeant, C. D. Incarvito, A. L. Rheingold, K. O. Hodgson, B. Hedman, E. I. Solomon and K. D. Karlin, *Inorg. Chem.*, 2007, **46**, 6056–6068.
20 G. Y. Park, Y. Lee, D.-H. Lee, J. S. Woertink, A. A. N. Sarjeant, E. I. Solomon and K. D. Karlin, *Chem. Commun.*, 2010, **46**, 91–93.
21 S. Itoh, *Curr. Opin. Chem. Biol.*, 2006, **10**, 115–122.
22 L. M. Mirica, X. Ottenwaelder and T. D. P. Stack, *Chem. Rev.*, 2004, **104**, 1013–1045.
23 E. A. Lewis and W. B. Tolman, *Chem. Rev.*, 2004, **104**, 1047–1076.
24 S. Itoh, in *Copper-Oxygen Chemistry*, ed. K. D. Karlin and S. Itoh, John Wiley & Sons, Hoboken, 2011, vol. 4, pp. 225–282.
25 R. L. Peterson, S. Kim and K. D. Karlin, in *Comprehensive Inorganic Chemistry II*, ed. J. Reedijk and P. K. Elsevier, Oxford, 2013, vol. 3, pp. 149–177.
26 A. Kunishita, M. Kubo, H. Sugimoto, T. Ogura, K. Sato, T. Takui and S. Itoh, *J. Am. Chem. Soc.*, 2009, **131**, 2788–2789.
27 A. Kunishita, M. Z. Ertem, Y. Okubo, T. Tano, H. Sugimoto, K. Ohkubo, N. Fujieda, S. Fukuzumi, C. J. Cramer and S. Itoh, *Inorg. Chem.*, 2012, **51**, 9465–9480.
28 A. W. Addison, T. N. Rao, J. Reedijk, J. van Rijn and G. C. Verschoor, *J. Chem. Soc., Dalton Trans.*, 1984, 1349–1356.
29 T. Tano, M. Z. Ertem, S. Yamaguchi, A. Kunishita, H. Sugimoto, N. Fujieda, T. Ogura, C. J. Cramer and S. Itoh, *Dalton Trans.*, 2011, **40**, 10326–10336.
30 T. Tano, H. Sugimoto, N. Fujieda and S. Itoh, *Eur. J. Inorg. Chem.*, 2012, **2012**, 4099–4103.
31 A. Kunishita, H. Ishimaru, S. Nakashima, T. Ogura and S. Itoh, *J. Am. Chem. Soc.*, 2008, **130**, 4244–4245.
32 D. D. Perrin, W. L. F. Armarego and D. R. Perrin, *Purification of Laboratory Chemicals 4th Edition*, Pergamon Press, Elmsford, NY, 4th edn, 1996.
33 M. G. Finn and K. B. Sharpless, *J. Am. Chem. Soc.*, 1991, **113**, 113–126.
34 A. Altomare, G. Cascarano, C. Giacovazzo, A. Guagliardi, M. Burla, G. Polidori and M. Camalli, *J. Appl. Crystallogr.*, 1994, **27**, 435–436.
35 M. C. Burla, R. Caliandro, M. Camalli, B. Carrozzini, G. L. Cascarano, L. D. Caro, C. Giacovazzo, G. Polidori, D. Siliqi and R. Spagna, *J. Appl. Crystallogr.*, 2007, **40**, 609–613.
36 S. Adachi, S. Nagano, K. Ishimori, Y. Watanabe, I. Morishima, T. Egawa, T. Kitagawa and R. Makino, *Biochemistry*, 1993, **32**, 241–252.
37 E. Baciocchi, M. Bietti, M. Salamone and S. Steenken, *J. Org. Chem.*, 2002, **67**, 2266–2270.